



Proof of NH₂-MWCNT/HRB nanocomposite as a revolutionary material in spacecraft: non-compromising improver in mass ratio and radiation shielding, and a growing relevance component in the aerospace and scientific community.

Neal Lobo #1, Riddhim Garg #2, Ebenezer Isaac K #3, Rayyan Sayed #4

Proof of NH₂-MWCNT/HRB nanocomposite as a revolutionary material in spacecraft: non-compromising improver in mass ratio and radiation shielding, and a growing in relevance component in the aerospace and scientific community.

Neal Lobo #1, Riddhim Garg #2, Ebenezer Isaac K #3, Rayyan Sayed #4

Incognito Blueprints Research Bootcamp 25

July 2023



Table of Contents

Abstract.....	3
1. Introduction.....	3
2. Materials and Methods.....	4
2.1.Tensile strength.....	4
2.1.1.Materials.....	4
2.1.1.1.Sample preparation.....	4
2.1.1.2.Experimental setup.....	5
2.1.1.3.Diameter measurement.....	5
2.1.2.Methods.....	5
2.1.2.1. Sample preparation.....	5
2.1.2.2.Experimental details.....	9
2.1.2.3. Tensile testing process.....	10
1. Diameter measurement.....	12
2.2.Thermal Radiation Shielding Capacity.....	12
2.2.1.Materials.....	12
2.2.2.Methods.....	13
2.2.2.1.Thermal analysis.....	13
3. Hypothesized Results.....	14
3.1.Tensile strength test.....	14
3.2.Thermal radiation test.....	15
4. Discussion.....	17
5. Conclusions & Future Outlook.....	21
5.1.The future outlook.....	21



5.2.Conclusion.....	21
Acknowledgments.....	22
Footnotes.....	22
Author contributions.....	22
Competing financial interests.....	22
References.....	23
Member Introduction.....	26

1. Introduction

Effective space radiation shielding is extremely crucial to the well-being of astronauts, to prevent them from serious health implications, such as immunity dysfunction, carcinogenesis, skin injuries, and more [1]. Spacecraft components are currently manufactured from aluminum owing to their cost-effectiveness and low weight. However, Aluminum performs poorly in providing effective spacecraft shielding against radiation [2]. Long and pure fibers of CNTs cannot be produced by typically used Chemical Vapor Deposition due to the limited amount of supply of catalyst that can be provided [3]. CNTs are polymerized with different materials such as epoxy resin to obtain long fibers. But in this process some properties like thermal radiation shielding capacity are compromised, which becomes a major concern for aerospace engineers [4]. Implementing the novel technology that Tuball has developed using the CNTs and using NH₂ - MWCNT/HRB nanocomposite as a radiation-shielding material in spacecraft, may prove more effective than present materials in missions with long-term exposure to thermal radiation. Its characteristic of being a low atomic number polymer will offer significant mass savings without compromising on any other mechanical properties like tensile strength. Keywords: NH₂- MWCNT/HRB nanocomposite, Radiation shielding, Thermal expansion, Tensile strength, Carbon nanotubes (CNTs).

2. Materials and Methods

This section will include experiments done to determine the tensile strength and thermal radiation shielding capacity of NH₂-MWCNT/HRB nanocomposite alongside MWCNTs.

2.1. Tensile strength

Tensile strength is one of the main factors in determining the usage of a material in the aerospace engineering sector, the higher the tensile strength of a material the better it is being employed in heavy load-carrying missions.

2.1.1. Materials

2.1.1.1. Sample preparation

Spinnable MWNTs were created using silicon wafers and semiconductor-grade Silicon substrates with a thermal oxide layer of 50 nm thickness and an iron catalyst coating of 2.5 nm produced by e-beam evaporation. A quartz reactor (4nm) was a crucial tool, and it was supplied with an acetylene concentration of 2.4% in helium (25 sccm in 1000 sccm He) [5]. A web of CNTs used in the experiment required graphite paint. From Tokyo Chemical Industry 3-Butoxyphenol, 1,12- diaminododecane and a 1 M sodium hydroxide aqueous solution. Chloroform from Alfa Aesar and paraformaldehyde from Sigma-Aldrich. Non-functionalized MWCNTs (pristine MWNCTs), amine-functionalized MWCNTs (NH₂-MWCNTs), and carboxylic acid-functionalized MWCNTs (COOH-MWCNTs) with outer diameters of 5-15 nm and lengths of 30-50 m are available from US Research Nanomaterials. The ASTM-D638 V-type epoxy specimen was created. Bisphenol A diglycidyl ether (epoxy equivalent weight of 186.9; Kukdo

Chemical) and 4'-diaminodiphenylmethane (Shuang Bang Industrial) were used to make the epoxy. The final material required is oven dried [6].

2.1.1.2.Experimental setup

2 piezoelectric actuators and 3 ultrasonic motors serves as the basis. Different elements were used independently: in the coarse movement, a carbon fiber shafts helped its development and in the fine movement, a close-ply stack type piezoelectric actuators and an extremely stable variable dc power supply were both necessary. A Field Emission Scanning Electron Microscope (FESEM) chamber (Philips XL30) was selected as the nano physical testing stage with an electron beam energy of 2KeV. An Atomic Force Microscope (AFM) tip strictly dependent on a X-piezo and a Z-piezo was ultimately listed [7].

2.1.1.3.Diameter measurement

A Transmission Electron Microscope (FEI Tecnai G2) grid is only needed in this phase [7].

2.1.2.Methods

2.1.2.1.Sample preparation

This study's NH₂-MWCNT/HRB nanocomposite was created as follows. According to the literature [8], 3-butoxyphenol, 1,12-diaminododecane, and paraformaldehyde were combined in chloroform (5 mL/g of reactants) in a mole ratio of 2:1:4.2. This reaction mixture was heated (57°C; bath) and agitated (600 rpm; Fig. 1 (a)), and the reaction product obtained was neutralised by sodium hydroxide (1 mol/L in water) and DI water (Fig. 1(b)). Anhydrous magnesium sulphate was added to the neutralised mixture in the earlier work [8] to dehydrate the chloroform component, which was subsequently filtered away. However, throughout the addition and filtration processes of our experiment, it was difficult to thoroughly filter anhydrous magnesium sulphate, and some contaminants from the filter contaminated the filtrate. When MWCNTs were sonicated with HRB dehydrated in chloroform, a fraction of the HRB was pre-cured by the heat created by the ultrasonic wave. To address these issues, the following MWCNT and HRB mixing stages were carried out. First, MWCNTs were introduced to chloroform and dispersed for roughly 30 minutes using a sonicator at 500 W and 20 kHz (40 mL of chloroform per 0.1 g of MWCNTs; Fig. 1 (d)). The resultant MWCNT dispersion was then combined with the neutralised mixture, agitated at 900 rpm in a 40 C bath, and evaporated until the volume was decreased to one-third of its original value (Fig. 1(e)). These techniques have also been proposed for dispersing MWCNTs in low-viscosity states. The viscosity of the MWCNT combination in chloroform is shown in Fig. 1(d). The resin precursor in Fig. 1(c) is also a low-viscosity liquid that is sufficiently mixed with chloroform, a tiny amount of neutralising solution, and HRB. As a result of combining these mixtures (Fig. 1(e)), MWCNTs were disseminated in HRB in a sufficiently low-viscosity state. According to the flowchart in Fig. 2, the resultant mixture (Fig. 1(e)) was put into a mould (Fig. 1(f)), and the

synthesised MWCNT/HRB nanocomposite was cured in a vacuum chamber (Fig. 1(g)). For the following reasons, the ideal HRB curing conditions were discovered by trial and error and empirical methodologies. The bubbles in the MWCNT/HRB structure produced before the curing burst when a high vacuum was created in the vacuum chamber. To address this issue, the bubbles were first eliminated under a low vacuum (10^{-2} Torr), and after 1 hour, a high vacuum pressure of 10^{-3} Torr was applied using a general vacuum pump. The bubble removal process became more intense as the temperature increased; thus, the temperature was gradually increased to totally eliminate all bubbles from the MWCNT/HRB composite. The ASTM-D638 standard was used to create a V-type specimen for a polymer tensile test (Fig. 1(h)) [6]. MWCNTs were produced as a forest on a silicon wafer using a chemical vapour decomposition (CVD) technique. This employed semiconductor-grade Silicon substrates with a 50 nm thermal oxide layer and a 2.5 nm iron catalyst coating produced by e-beam evaporation. With a running time of 10 minutes and a temperature of 680 C, an acetylene concentration of 2.4% in helium (25 sccm in 1000 sccm He) was supplied into a 44 mm id quartz reactor. More information about this procedure can be found elsewhere [5]. Vertically aligned MWNTs in the forest can be woven into a web of CNTs, which is the primary assessment indicator for carbon nanotube spinnability [9]. The web was created by plunging the sharp edge of a scalpel into the forest and then peeling it away horizontally. The forest CNTs string out behind the scalpel and stay together without the presence of a binding agent. The CNT web was put onto a thin coating of graphite paint to create the test samples. After drying, a second layer of paint was applied to the web. The samples were then oven-dried for 30 minutes at 350°C to completely dry the paint and evaporate the polymer binder. The CNT web and graphitic film were then combined to produce a very thin layer that was pulled apart,

revealing the MWCNTs projecting from the edge. The torn film was placed in the experimental apparatus and served as the source of the MWCNT specimens that were evaluated [7].

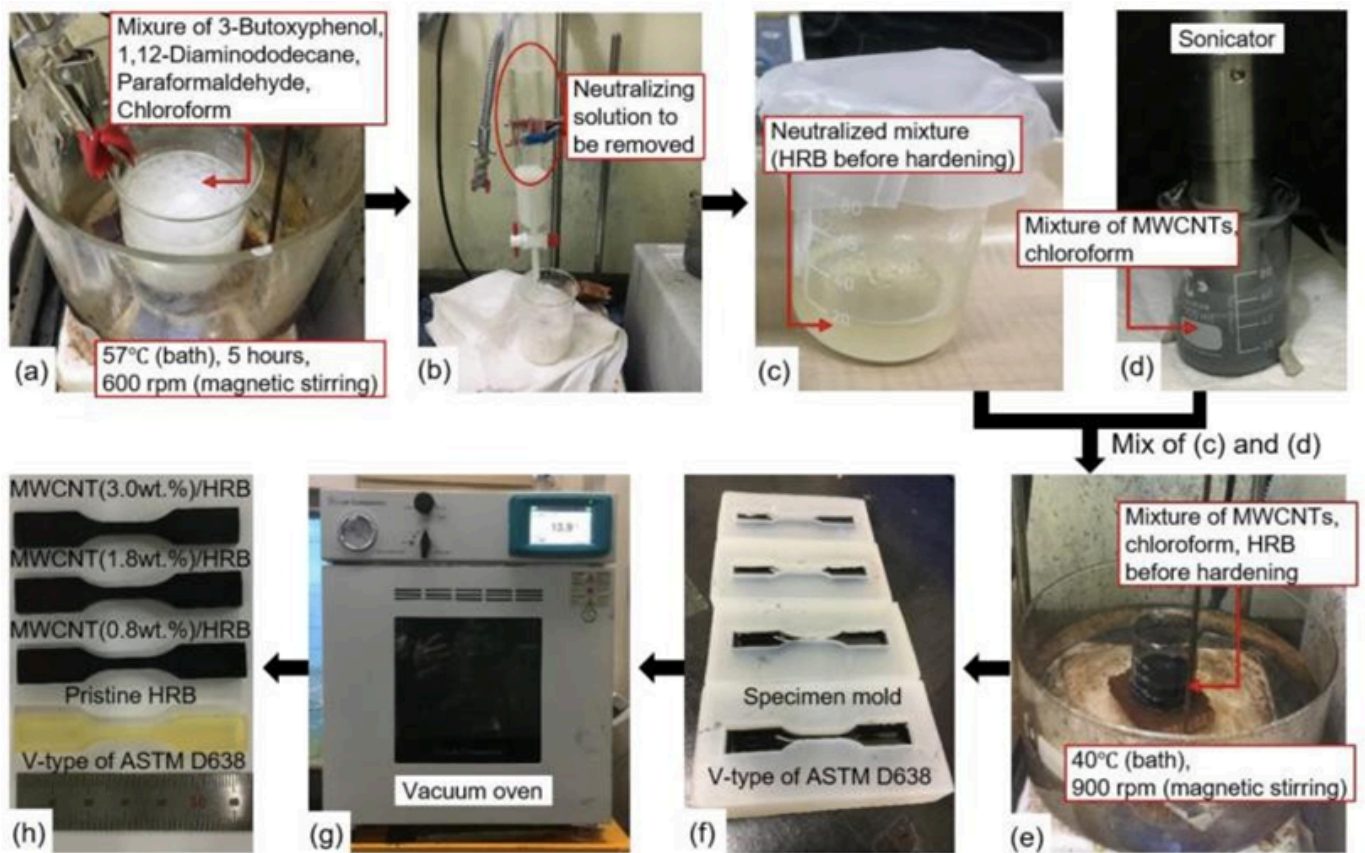


Fig. 1. MWCNT/HRB nanocomposite manufacturing steps.

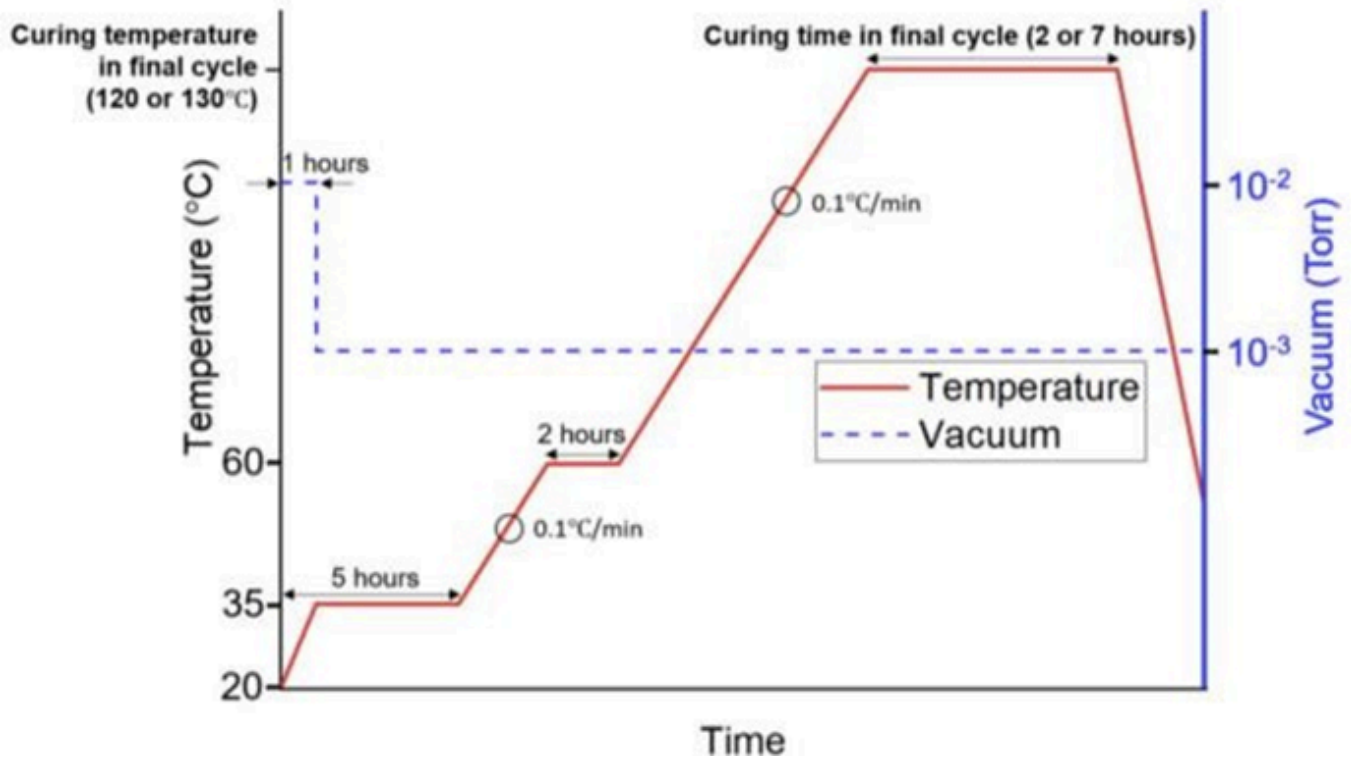


Figure 2. Temperature, time, and vacuum profiles of HRB manufacturing performed in the vacuum oven.

2.1.2.2. Experimental details

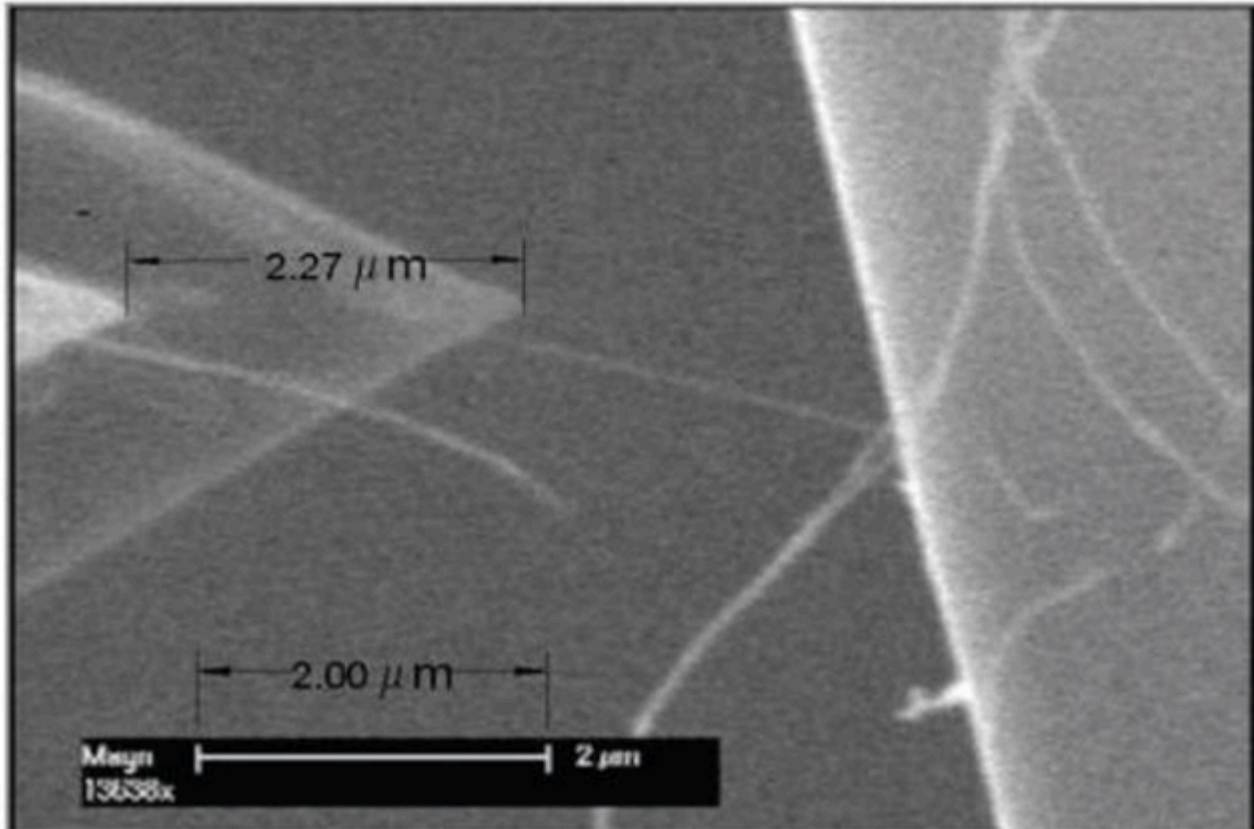
The approach previously proposed by [9,10] is extended here to measure the strength of multiwalled carbon nanotubes. Tensile testing was performed on MWCNTs in a nano physical testing stage that includes two piezoelectric actuators and three ultrasonic motors. This stage's movement can be divided into two phases: "coarse movement" and "fine movement." Ultrasonic linear friction motors with carbon fibre shafts may provide coarse movement in the X, Y, and Z directions. To maintain or vary locations, close-ply stack-type piezoelectric actuators in the X and Z directions were used, together with an exceptionally stable variable dc power supply. The tip of an Atomic Force Microscope (AFM) was linked to the X-piezo. On the Z-piezo, the CNT sample and the reference AFM tip were put. To collect and evaluate the CNT, the AFM tip was moved in coarse (X, Y, and Z directions) and fine (X and Z directions). The

entire nano physical testing stage was carried out inside a Philips XL30 Field Emission Scanning Electron Microscope (FESEM) chamber. To avoid the formation of amorphous carbon on the test samples, the electron beam energy in the SEM was limited to a minimum of 2 keV. Each trial was videotaped, and the data was analysed when the video frame images were converted to computer files [7].

2.1.2.3. Tensile testing process

The functioning AFM tip, which was linked to an X-piezo, served as both a nano manipulator and a force sensor. The AFM tip was employed as a nano manipulator to collect the CNT specimen from the sample. The working AFM tip was calibrated against a reference AFM tip installed on the stage that had been pre-calibrated by measuring the cantilever beam's resonance frequency and combining it with the Euler-Bernoulli beam theory [11,12]. To calibrate the working AFM cantilever, it was placed on top of the reference AFM cantilever, and the deflections of both were measured at various points. The applied force will be of identical magnitude but opposite direction. As a result of knowing the spring constant of the reference AFM tip ahead of time and measuring the deflections of both AFM tips, the spring constant of the working tip may be computed. It was assumed in this operation that the spring constants of both cantilevers were unaffected by the direction of the force or the minor displacement used in the experiment. The spring constant of the working AFM cantilever used in the first experiment was 0.29 N/m and 0.42 N/m in the second. Individual MWNTs were attached to the probe via in situ deposition of amorphous carbon via extended scanning of the microscope's electron beam. After guiding the AFM tip to make contact with a single CNT, the

beam was focused solely on the point of contact for many minutes. The electron beam destroyed traces of carbonaceous vapour in the SEM environment that had collected as carbon on the sample as it rested on the probe, effectively welding it in place. After that, each specimen was gradually stress-loaded through the probe by retracting the piezo actuator while SEM was used to observe the process. Fibres were either ripped free from the graphite film and transported to and welded onto a TEM grid, which is also installed on the Z piezo for testing, or the fibres snapped and the force to break was recorded. If there was still enough fibre on the AFM tip after the initial break, the distal end was positioned on the TEM grid, welded, and the fibre was examined again. One fibre was successfully tested in a total of 16 attempts using this method and relocating the fractured fragments. Each test was video recorded, and the displacement of the probe up to the failure of the CNT was measured. As a result, in these studies, the AFM probe served as a force transducer, measuring force as a function of displacement. To decrease noise, the video capture contained an 8-frame averaging method. The essential displacement data is provided by this overlay image (Figure 3) in conjunction with the data bar produced by the SEM. The strength of the CNT is calculated using the force constant of the AFM cantilever probe and the diameter of the CNT [7].



Figure

3: Superimposed video frames for force measurement.

2.1.2.4. Diameter Measurement

The sizes of the CNTs employed were estimated using a Transmission Electron Microscope (FEI Tecnai G2). It was difficult to position the samples on the TEM grid and then move them from the SEM to the TEM due to the amount of amorphous carbon accumulating on the CNTs attached to the TEM grid employed. As a result, diameters were calculated by measuring a large number of pristine CNTs at random from the same forest that was used to prepare specimens for the experimental strength tests. The electron beam energy was kept as low as possible during TEM imaging to avoid sample damage and amorphous carbon buildup [7].

2.2. Thermal Radiation Shielding Capacity

One of the most important things to keep in mind while making any spacecraft is its resistance against the harsh space environment, one of which includes its capacity to withstand different radiations like cosmic radiation, thermal radiation, etc. The spacecraft should be able to tolerate these brutal conditions so that is why employment of a material which can withstand these conditions without affecting the spacecraft becomes necessary.

2.2.1. Materials

A scanning calorimeter (DSC, TA Q 1000) capable of thermal analysis and a Dynamic Mechanical Analyzer (DMA-7, Perkin Elmer) according to the specifications, ASTM Standard D4065 capable of determine the coefficient of thermal expansions cover great part of this section. Lastly, a 1,3- phenylenediamine (mPDA) cured diglycidyl ether of bisphenol A (EPON 828) and a thermo- mechanical analyzer (TMA, SDTA840) were needed [13].

2.2.2. Methods

2.2.2.1. Thermal analysis

The thermal study was carried out in a nitrogen atmosphere using a differential scanning calorimeter (DSC, TA Q1000) at a flow rate of 50 cc/min. The curing reaction of the resins with

and without CNTs was carried out at a heating rate of 10 C/min from ambient to 300 C. The thermomechanical characteristics were determined using an ASTM Standard D4065-compliant dynamic mechanical analyzer (DMA-7, Perkin Elmer). In a nitrogen atmosphere, samples 20 mm long, 3 mm wide, and 1 mm thick were loaded in three-point bending from ambient to 300 C at a heating rate of 5 C/min and a frequency of 1.0 Hz. Using a thermo-mechanical analyzer (TMA, SDTA840), the CTEs were calculated directly from the slopes of the linear areas of the sample thickness change vs temperature curves at temperatures both below and above T_g . CTEs for CNT/epoxy composites produced from 1,3-phenylenediamine (mPDA) cured diglycidyl ether of bisphenol A (EPON 828) were also found [13].

3. Hypothesized Results

3.1. Tensile strength test

Before tensile strength testing could begin, multiple samples of MWCNTs were used to measure the diameter of the CNTs that were to be experimented on. A sample image was used as a reference template along with the constant wall spacing of 0.34 nm to carry out diameter and wall thickness measurements. The sample under testing had 6 walls thus the thickness was calculated to be 2.04 nm. Furthermore, the outer diameter of the CNT samples was found to be 10.77 ± 1 nm. The testing of these spinning CNTs under constant duress was evaluated on the assumption that the MWCNTs were perfectly cylindrical. The results calculated by N. Khandoker et al in [7] showed that the strength of these spinning CNTs can

be anywhere between 20 to 90 GPa with a mean of 48 GPa under the assumption. Since the nanotube walls themselves are only held together by relatively weak Van der Waals forces, when a hollow cylindrical MWCNT was considered, the mean value of the tensile strength jumped to 378 GPa [7].

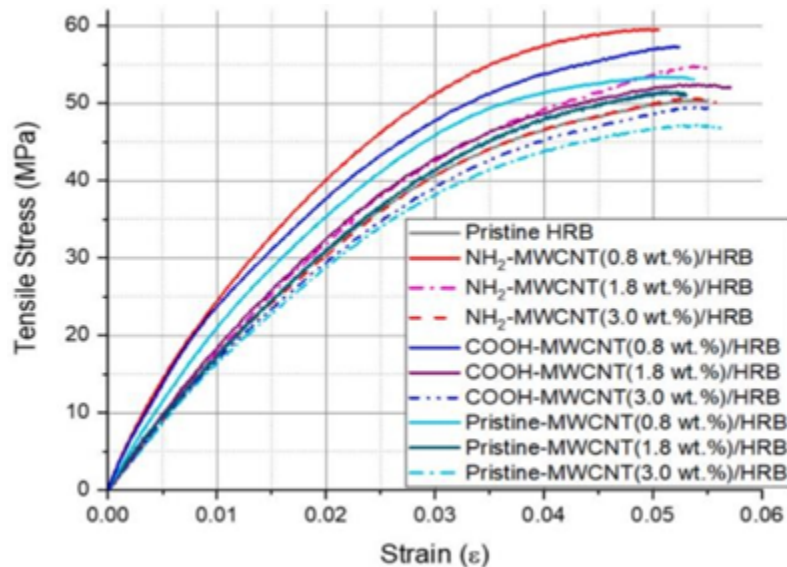


Figure 4. Tensile strength test results of various different functionalized nanocomposites

This graph was produced by J.-H. Cha et al. [6] in which we can see the red line depicting tensile strength of NH₂-MWCNT/HRB nanocomposite is clearly higher than all other MWCNT composites with different CNT wt% configurations. Functionalized CNTs, like the NH₂ functionalized MWCNT/HRB nanocomposite we are using, increase mechanical properties and significantly increase the nanocomposite's strength [13].

3.2. Thermal radiation test

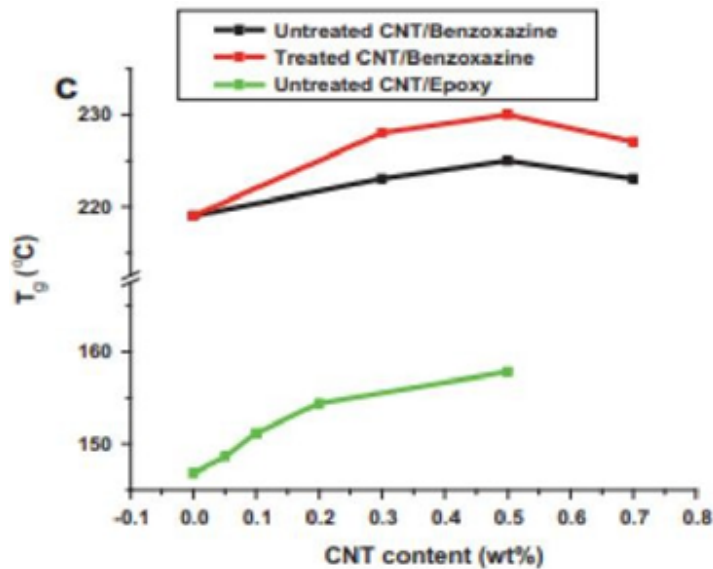


Figure 5: Glass transition temperature versus CNT wt% content comparing treated and untreated CNT nanocomposites

Glass transition temperature (T_g) is an important factor to be measured when using polymers such as MWCNTs for all applications. This particular characteristic of polymers becomes more crucial when considering the fact that the MWCNTs are going to be under constraint stress and face extreme temperatures in the space environment. A viable T_g would assure the MWCNT's proper functionality once in space. As mentioned earlier, the benzoxazine resin was mixed with CNTs, specifically MWCNTs. What was observed was that the onset and maximum exothermic temperature decreased substantially [13]. In addition, J.-H. Cha et al. also discuss similar results in [6] where the MWCNTs increase the degree of intramolecular curing of HRB (a common type of benzoxazine) resulting in improved thermomechanical properties. M. Kaleemullah et al. also mention that the presence of CNTs decreases mobility

thus resulting in a higher glass transition temperature (T_g). It is also tested that at temperatures around 50-150 degree Celsius, treated CNTs combined with a benzoxazine resin had the highest tensile strength ranging from 3.75 to 4.50 GPa. Not only that but in Figure 7c in [13] you can also see that the treated CNT/Benzoxazine nanocomposite had the highest glass transition temperature, T_g , at around a 0.5 wt% CNT content.

Materials	Onset temp. T_{onset} (°C)	Max temp. T_m (°C)	T_g (°C)	Enthalpy (ΔH) (J/g)
<i>Group A</i>				
Neat resin	243.0	255.2	201	365.7
0.3 wt.% Untreated CNTs	241.7	254.2	206	337.3
0.5 wt.% Untreated CNTs	238.1	249.8	208	298.9
0.7 wt.% Untreated CNTs	237.6	249.0	208	297.3
<i>Group B</i>				
0.3 wt.% Treated CNTs	240.3	253.5	207	354.2
0.5 wt.% Treated CNTs	237.2	251.2	209	342.9
0.7 wt.% Treated CNTs	236.4	250.2	210	338.6

Figure 6: Glass transition temperature versus CNT wt% content comparing treated and untreated CNT nanocomposites

4. Discussion

Individual multi-walled Carbon Nanotubes (CNTs) are extremely strong and rigid. The experimental tensile strength of spinnable multi-walled carbon nanotubes (MWNT) is reported in this work. The fracture strength was computed using the applied force and the CNT diameter. Fracture strength is investigated in connection to the number of failed walls, pullout behaviour, and angle of stress. The tensile strength of the tested spinnable CNTs ranged from

20 to 90 Gpa, with a mean value of 48 Gpa when considering a solid cross-sectional area. CNT structure promises exceptional properties such as strength, stiffness, conductivity, connectivity, surface area, and physical and chemical stability for applications ranging from single nanotube-based electronics to lift cables to orbit, from bio-sensors to composites for aerospace and automotive structures. However, neither pure bulk nor composite applications aiming at leveraging their strength have been able to demonstrate this capability on a macroscopic scale. CNTs, as a pure bulk material, are perfect for creating ultra-high strength yarns for load and electrical current carrying applications. Fibrous materials are commonly employed as reinforcement fillers in composites. The theoretical strength of the CNTs, the way genuine individual CNTs fail, and the processes by which CNTs interact with one other and the surrounding matrix may all contribute to the high aspect ratio. As a result, many experimental and theoretical research have focused on evaluating and analysing the behaviour of carbon nanotubes under tensile pressure. CNTs' microscopic dimensions, with diameters in the nanometre range and lengths in the hundreds of micron range, place severe limitations on how they may be observed and handled [7].

We expand the usage of the approach proposed earlier by [10, 14] to measure the strength and modulus of multiwalled carbon nanotubes in the vicinity of 100 GPa and 1 TPa, respectively, and this is broadly corroborated by practical measurements of isolated SWNTs and MWNT outer shells. This implies that CNT production and processing were major determinants in their mechanical properties.

Carbon nanotubes (CNTs) have piqued the interest of researchers as a reinforcement for polymer-matrix composites due to their unique structural and transport features, such as outstanding modulus and strength, high electrical and thermal conductivities, and great chemical stability, as well as their low densities [15-17]. The mechanical and thermomechanical characteristics of poly benzoxazine nanocomposites including functionalized multi-walled carbon nanotubes (MWCNTs) are investigated. The findings are explicitly compared to the characteristics of epoxy-based nanocomposites. CNTs improve CNT/polybenzoxazine nanocomposites' flexural strength, flexural modulus, storage modulus, and glass transition temperature, T_g , at the expense of impact fracture toughness. Surfactant treatment improves these properties, with the exception of impact toughness, by increasing CNT dispersion and interfacial contact. In general, the former four parameters are higher for CNT/polybenzoxazine nanocomposites than for epoxy counterparts, and vice versa for impact toughness. The addition of CNTs improves the coefficient of thermal expansion (CTE) of polybenzoxazine nanocomposites in both regions below and above T_g , whereas the opposite is true for epoxy nanocomposites. This finding has implications for using CNT/poly benzoxazine nanocomposites in applications needing low shrinkage and precise dimensional control [13].

Many advantages exist for epoxy resins, including superior mechanical qualities, high impact resistance and minimal creep, good adhesive properties, resistance to environmental degradation and chemicals, good dielectric properties, and wear resistance [18]. However, they have drawbacks such as high volumetric shrinkage after curing, low heat resistance, short shelf life, poor oxidative stability, and moisture sensitivity [19].

CNT/polybenzoxazine nanocomposites were created with and without surfactant treatment of the CNTs. The mechanical and thermomechanical properties of the nanocomposites were examined in detail and compared to those of epoxy nanocomposites. The following are the major conclusions from this study[13]:

- I. The flexural modulus and strength of polybenzoxazine nanocomposites including treated CNTs exceeded those of untreated CNT nanocomposites and epoxy nanocomposites.
- II. Regardless of CNT functionalization, the impact fracture toughness of CNT/polybenzoxazine nanocomposites decreased with increasing CNT content. The epoxy-based nanocomposites displayed a substantially higher fracture toughness and a reversed trend in terms of CNT concentration than the polybenzoxazine equivalent.
- III. The storage modulus and glass transition temperature of CNT/poly benzoxazine nanocomposites increased with CNT concentration and were significantly higher than those of CNT/epoxy nanocomposites. Both characteristics were significantly improved by CNT functionalization.
- IV. The CNT/polybenzoxazine nanocomposites outperformed the epoxy equivalent in terms of dimensional stability as assessed by CTE below T_g . The CTE of the former composites dropped continuously as CNT content increased, but the opposite is true for the latter composites.

However, in order to effectively leverage the extraordinary capabilities of carbon nanotubes in a polymer composite, the carbon nanotubes must be properly disseminated and individualised within the matrix. Because of the inherent intertube van der Waals forces, CNTs tend to cluster into bundles or ropes. The existence of these bundles significantly reduces the CNT/matrix interfacial surface area. As a result, the maximum load transfer feasible to the nanotube network is lowered [20].

In comparison to the large number of investigations on epoxy and CNT nanocomposites, the coupling of CNTs with benzoxazine is a relatively recent topic in materials science. Nonetheless, benzoxazine resins appear to have some significant advantages because their primary structure appears to favour facile dispersion of CNTs without the use of a surface functionalizing agent. Indeed, employing a sonication probe, for example, a uniform dispersion condition may be easily established, and the resulting nanocomposites display electrical percolation thresholds at low concentrations of CNTs (less than 0.5 wt%). This review further emphasises that the structure of the monomer is critical for the creation and maintenance of strong CNT/polymer contacts during network cross-linking. Most benzoxazine monomers have good interactions with CNTs, but only a few of them retain them cross-linked. The reasons are yet unknown and require a more in-depth experimental as well as theoretical approach for a clear understanding. Even though the physical properties of CNTs are altered to some extent, the covalent bond between CNTs and benzoxazine resin appears to offer certain advantages. In the case of BA-a resin, for example, no evident property changes are noticed with the introduction of pure CNTs, but functionalized ones are shown to improve

thermo-mechanical stability after curing. The fundamental restriction of chemical functionalization is the comparatively limited number of effective covalent bonds formed. Alternative reactions using maleimide, furan, or acrylonitrile groups are likely to be more interesting because to their potential interaction with the surface of CNTs. Finally, the major idea to take away from this chapter is that the use of benzoxazine with carbon nanotubes allows for the development of nanocomposites or nanohybrids with unique and exceptional features, making them promising candidates for the next generation of composite materials [20].

5. Conclusions & Future Outlook

5.1.The future outlook

The future usage of NH₂-MWCNT/HRB nanocomposite and MWCNTs includes their major employment in the aerospace sector. These materials with high tensile strength have great potential to be used in heavy machinery so as to increase strength and still the machine being lightweight. The future beholds versatile uses of these materials and these may be used in a way that these were not originally designed to be and may open doors to various opportunities in the scientific world one of which may be the space elevator.

5.2.Conclusion

To sum up, the aim of this report was to showcase the potential not yet fulfilled of the NH₂-MWCNT/HRB nanocomposite in the spacecraft industry. Down to its composition, it is explicit the possibility of mass improvements in aspects such as maneuverability, mechanical properties and thermal radiation shielding capacity regarding its novelty against out-dated, commonly used components such as epoxy and aluminum with great impact on the market. This seemingly asset also brings new challenges in the scientific community considering the lack of experimentation concerning the compatibility of this technology and its range of applications. In spite of this fact, the outlook is positive and this report is proof of the soon expanding spacecraft technologies due to components such as this one.

Acknowledgments

The research in this report was initiated and supported by Incognito Blueprints. We thank our TA/advisor Mr. Aniruddh for guidance throughout the research.

Footnotes

R. Sayed worked out the introduction, R. Garg proposed experiments in the methods section, raised the future outlook, and compiled the materials needed, N. Lobo conceived and recorded the hypothesized results and wrote the conclusion. E.K. Isaac came up with the discussion.

Competing financial interests

The authors declare no competing financial interests.

References

1. J.C. Chancellor, G.B. Scott, J.F. Sutton, "Space Radiation: The Number One Risk to Astronaut Health beyond Low Earth Orbit," *Life (Basel)*, 4(3), pp. 491- 510, Sep 2014.
2. Z. Li, S. Nambiar, W. Zheng, J.T.W. Yeow, "PDMS/single-walled carbon nanotube composite for proton radiation shielding in space applications," *Materials Letters*, 108(2013), pp. 79-83.
3. N. M. Mubarak, E. C. Abdullah, N. S. Jayakumar, and J. N. Sahu, "An overview on methods for the production of carbon nanotubes," *Journal of Industrial and Engineering Chemistry*, vol. 20, no. 4, pp. 1186–1197, Jul. 2014, doi: <https://doi.org/10.1016/j.jiec.2013.09.001>.
4. V. K. Srivastava, "Modelling and mechanical performance of carbon nanotube/epoxy resin composites," *Materials & Design*, vol. 39, pp. 432–436, Aug. 2012, doi: <https://doi.org/10.1016/j.matdes.2012.02.039>
5. Huynh, C.P., et al., Evolution of directly-spinnable carbon nanotube growth by recycling analysis. *Carbon (Inpress)*, 2011.

6. J.-H. Cha, W.-H. Jang, S. K. Sarath Kumar, J.-E. Noh, J.-S. Choi, and C.-G. Kim, “Functionalized multi-walled carbon nanotubes/hydrogen-rich benzoxazine nanocomposites for cosmic radiation shielding with enhanced mechanical properties and space environment resistance,” *Composites Science and Technology*, vol. 228, p. 109634, Sep. 2022, doi: <https://doi.org/10.1016/j.compscitech.2022.109634>.
7. N. Khandoker, S. C. Hawkins, R. Ibrahim, C. P. Huynh, and F. Deng, “Tensile Strength of Spinnable Multiwall Carbon Nanotubes,” *Procedia Engineering*, vol. 10, pp. 2572–2578, Jan. 2011, doi: <https://doi.org/10.1016/j.proeng.2011.04.424>.
8. D. Iguchi, S. Ohashi, G.J.E. Abarro, X. Yin, S. Winroth, C. Scott, M. Gleydura, L. Jin, N. Kanagasegar, C. Lo, C.R. Arza, P. Froimowicz, H. Ishida, Development of hydrogen-rich benzoxazine resins with low polymerization temperature for space radiation shielding, *ACS Omega* 3 (2018) 11569–11581, <https://doi.org/10.1021/acsomega.8b01297>.
9. Chi P. Huynh and S.C. Hawkins, Understanding the synthesis of directly spinnable carbon nanotube forests. *Carbon* 2010. 48: p. 1105-1115.
10. Yu, M.-F., et al., Strength and Breaking Mechanism of Multiwalled Carbon Nanotubes Under Tensile Load. *Science*, 2000. 287(5453): p. 637-640.
11. Cleveland, J.P., et al., A nondestructive method for determining the spring constant of cantilevers for scanning force microscopy. *Rev. Sci. Instrum.* , 1993. 64(2): p. 403-405.
12. Sadara, J.E., J.W.M. Chon, and P. Mulvaney, Calibration of rectangular atomic force microscope cantilevers. *Review of Scientific Instruments* 1999. 70(10).

13. M. Kaleemullah, S. U. Khan, and J.-K. Kim, "Effect of surfactant treatment on thermal stability and mechanical properties of CNT/polybenzoxazine nanocomposites," *Composites Science and Technology*, vol. 72, no. 16, pp. 1968–1976, Nov. 2012, doi: <https://doi.org/10.1016/j.compscitech.2012.08.020>.
14. Deng, F., T. Ogasawara, and N. Takeda. Microscopic dynamic observation and experimental characterization of carbon nanotubes Poly ether ether ketone composites. in Twelfth US-Japan conference on composite materials.
15. Thostenson E, Ren Z, Chou TW. Advances in the science and technology of carbon nanotubes and their composites: a review. *Compos Sci Technol* 2001;61:1899–912.
16. Xie XL, Mai YW, Zhou XP. Dispersion and alignment of carbon nanotubes in polymer matrix: a review. *Mater Sci Eng: R: Rep* 2005;49:89–112.
17. Thostenson ET, Lee CY, Chou TW. Nanocomposites in context. *Compos Sci Technol* 2005;65:491– 516.
18. Shalin RE. Epoxy matrices polymer matrix composites. London: Chapman & Hall; 1995. 11– 34.
19. Rosato DV, Rosato MG, Rosato DV. Epoxy plastics concise encyclopedia of plastics, vol. 237 Boston: Kluwer Academic Publishers; 2000.
20. L. Dumas, L. Bonnaud, and P. Dubois, "Chapter 38 - Polybenzoxazine Nanocomposites: Case Study of Carbon Nanotubes," *ScienceDirect*, Jan. 01, 2017.

